Supplementary Material (ESI) for Chemical Communications

Time-resolved UV-visible spectroelectrochemistry using 3D-transparent mesoporous nanocrystalline ITO electrodes

Christophe Renault,[a] Ken D. Harris,[b] Michael J. Brett,[c] Véronique Balland*[a] and Benoît Limoges*[a]

[a] *Laboratoire d'Electrochimie Moléculaire, Université Paris Diderot, UMR CNRS 7591, 15, rue Jean-Antoine de Baïf, 75205 Paris Cedex 13, France.*

[b] *National Research Council (NRC), National Institute for Nanotechnology (NINT), Edmonton, Alberta, Canada T6G 2M9.*

[c] *Electrical and Computer Engineering, University of Alberta, Edmonton, Alberta, Canada T6G 2V4.*

1. Experimental section

All chemicals, including microperoxidase 11, were purchased from Sigma-Aldrich and used without further purification. Aqueous solutions were prepared with milli-Q water obtained from a Millipore purification system. Microperoxidase 11 solution were prepared in HEPES buffer (50 μM, pH 7.0) and its concentration was determined by UV-visible spectroscopy using ε_{404} = 95 $mmol^{-1}$ L cm^{-1}.

ITO electrode preparation. The ITO substrates were deposited by electron beam evaporation in a glancing angle deposition (GLAD) process. Source ITO material (91% In_2O_3, 9% SnO_2) was purchased from a commercial source (Cerac) and was used without further purification. A 20-25 mA electron beam current was accelerated at 9.0 kV to produce a deposition rate of 0.1-0.15 nm s^{-1} as detected by a quartz crystal microbalance situated at a normal deposition angle. The pressure during deposition was approximately 1.5 × 10^{-5} torr. Thickness of 200 nm of ITO were deposited while the substrates were maintained at a constant glancing angle of α = 75° and rotated through five complete revolutions to achieve a high surface area, vertical posts microstructure. Immediately following deposition, the ITO films were non-transparent and modestly conductive, and therefore, a post-process anneal procedure was implemented to improve these properties. The samples were first annealed in an air environment at 500°C for 90 minutes to incorporate oxygen and improve crystallinity, followed by a second anneal at 375°C for 60 minutes in a forming gas (H_2/N_2) environment. Following this treatment, the samples are highly transparent, and excellent conductivity is achieved.

Once prepared, the substrates were cut in rectangular pieces of ~1 × 1 cm^2 or ~0.8 × 2.5 cm^2 for UV-visible experiments or UV-visible spectroelectrochemical measurements, respectively. With the aim to have a well-defined working electrode area during spectroelectrochemical experiments, an electroactive area of 0.8 cm^2 was delimited at the extremity of the ITO rectangular piece with an insulating layer of varnish.

UV-visible spectroelectrochemistry. Spectroelectrochemistry was performed in a home-made one-compartment three-electrode cell. A DRIREF Ag/AgCl, KCl (3 M) reference electrode (World Precision Instrument) and a platinum wire (1-mm diameter) were used as reference and auxiliary electrode, respectively. The three electrodes were inserted into a 1-cm path length quartz cell through a silicon cap that hermetically closes the cell. An additional tygon tube for degassing was introduced. The spectroelectrochemical cell was filled with 1.5 mL buffer, continuously purged with argon during the entire experiment and thermostated to 20°C. The working electrode is the ITO substrate with an electroactive area of 0.8 cm^2. All experiments were carried out in an aqueous medium buffered with 100 mM HEPES at pH 7.0.

Cyclic voltammetry measurements were performed with an Autolab potentiostat, PGSTAT 12 (Ecochemie) interfaced to a PC computer (GPES software) with ohmic drop compensation. UV-visible absorption spectroscopy was carried out on a HR2000+ spectrometer (Ocean Optics) equipped with a balanced deuterium tungsten source (Micropack). The cell was thermostated to 20°C using a Peltier-controlled cuvette holder (Quantum Northwest). Integration time was fixed to 20 ms except for rapid scan measurements of Fig S4 for which an integration time of 4 ms was used.

Derivative cyclic votabsorptogram (DCVA) were calculated from the cyclic voltabsorptogram after applying a Fourier transform smoothing algorithm. The DCVAs were expressed in flux density by using equation 1:

$$\Phi = \frac{dA_{420}}{\Delta\varepsilon_{420} dt} = \frac{v dA_{420}}{\Delta\varepsilon_{420} dE} = \frac{i}{nFS} \qquad (1)$$

Where Φ is the flux density (mol cm^{-2} s^{-1}), A_{420} is the absorbance monitored at 420 nm, $\Delta\varepsilon_{420} = \varepsilon_{red} - \varepsilon_{ox}$ = 42 000 mol^{-1} L cm^{-1} is the difference in molar extinction coefficient of the reduced and oxidized form of the MP-11, v is the scan rate, E the applied potential, n the number of electron involved in the electrochemical reaction, F the Faraday constant and S the effective geometric electrode area.

2. Figures

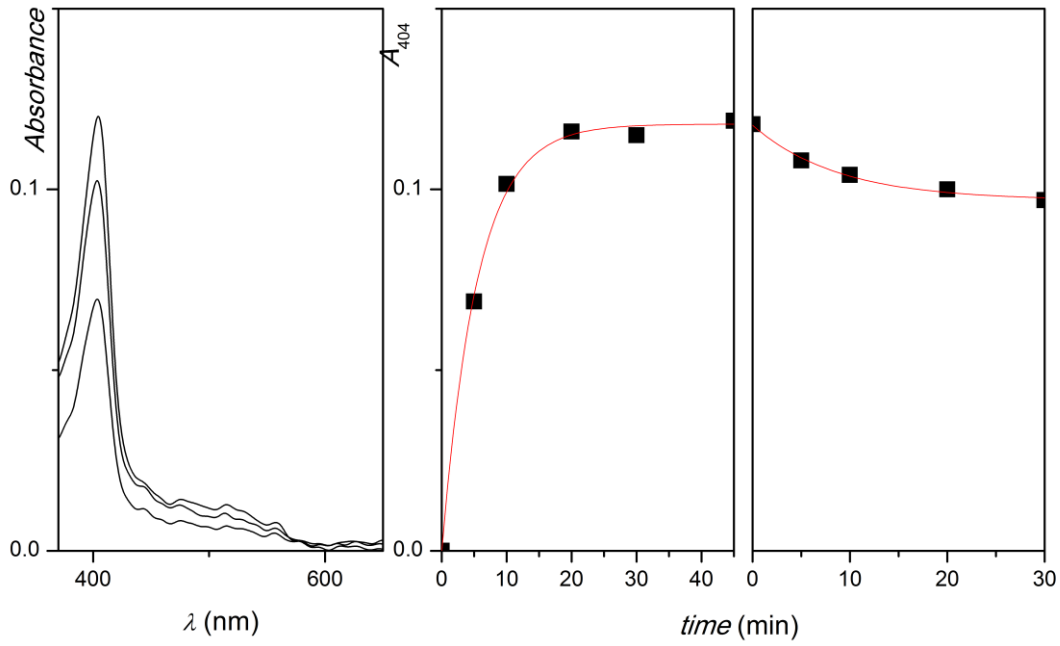

Figure S1: (Left) UV-visible absorption spectra recorded after 5, 10 and 45 min for a mesoporous ITO electrode soaked into a 50 μM MP-11 solution (10 mM HEPES, pH 7.0). Each reported spectra is the averaging of 256 spectra recorded each with an integration time of 20 ms. (Right) Plots of the absorbance monitored at 404 nm as a function of adsorption and desorption time (i.e., in a protein-free buffer of 10 mM HEPES, pH 7.0). The adsorption kinetic was fitted (red line) to a pseudo one-order kinetic with an apparent rate constant k_{ads} = 0.18 min^{-1}. T = 20°C.

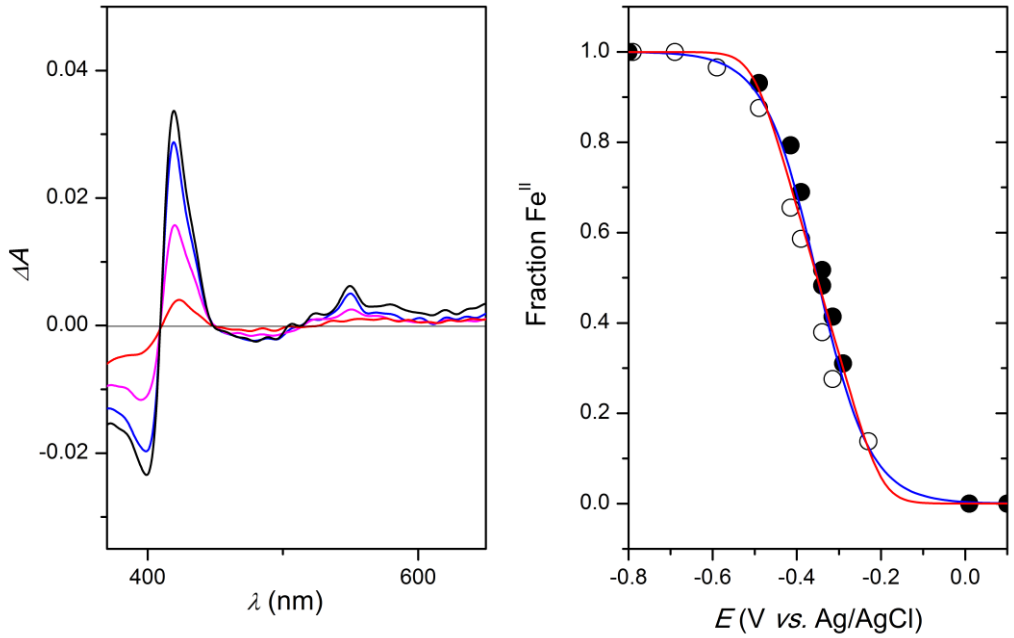

Figure S2: Left: difference spectra recorded during the spectroelectrochemical titration of MP-11 adsorbed within the ITO thin film at (red) -0.25, (magenta) -0.35, (blue) -0.45 and (black) -0.7 V *vs.* Ag/AgCl. Each reported spectra is the averaging of 256 spectra recorded each with an integration time of 20 ms. Right: fraction of reduced MP-11 determined from the 420 nm absorbance during reductive (○) and oxidative (●) titrations. Blue line: Nernst fitting using n = 0.4 and $E^{0'}$ = -0.35 V. Red line: fit based on a square distribution of $E^{0'}$ and n = 1 (see eq 3 in reference 21). T = 20°C; 100 mM HEPES buffer, pH 7.0.

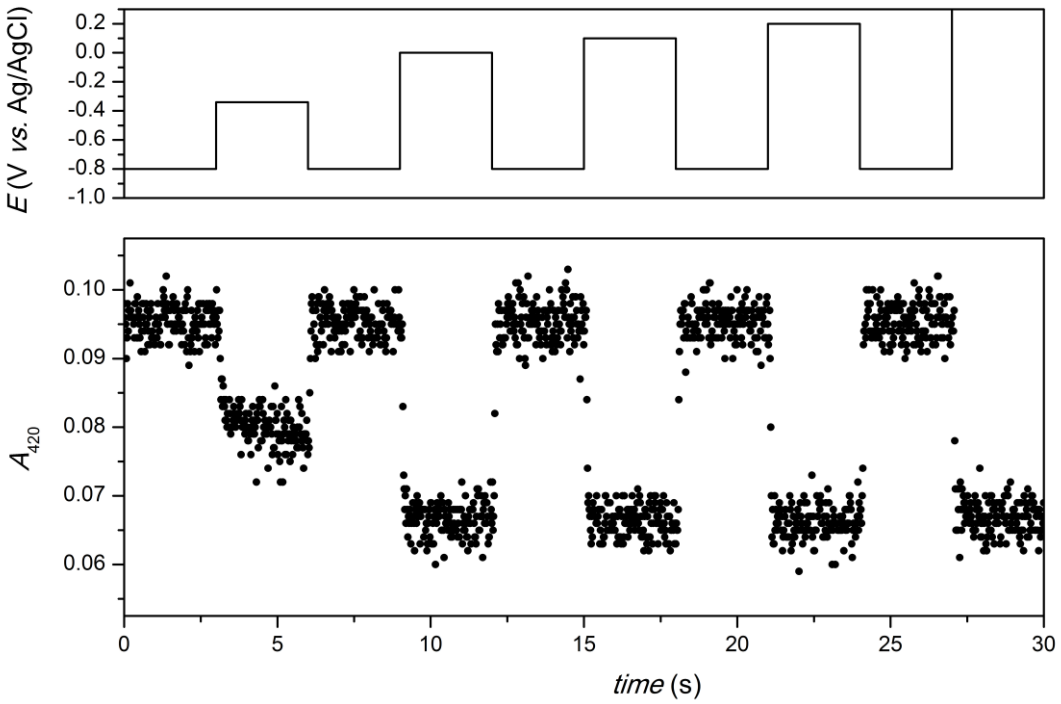

Figure S3: Absorbance (●) of a mesoporous ITO electrode loaded with MP-11 ($\Gamma = 8 \times 10^{-10}$ mol cm^{-2}) and monitored at λ = 420 nm during a series of normal pulse potential steps (black line) from -0.8 to -0.34, 0, 0.1, 0.2 and 0.3 V *vs.* Ag/AgCl. Integration time: 20 ms; T = 20°C; 100 mM HEPES buffer, pH 7.0.

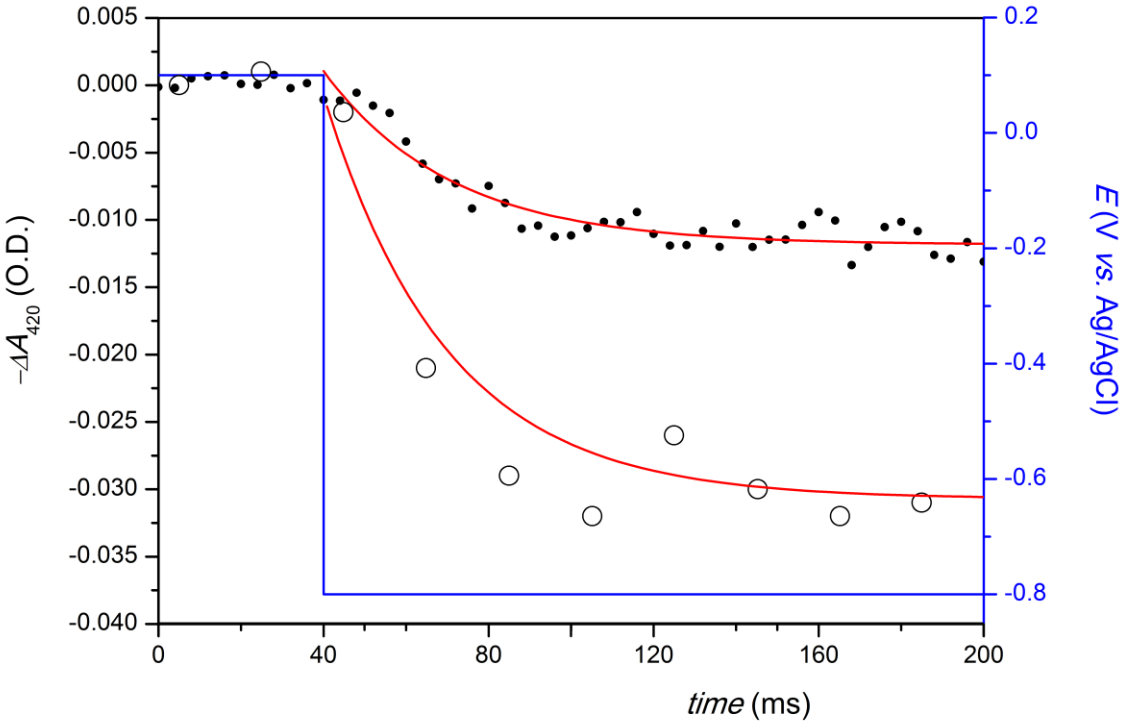

Figure S4: Absorbance of a mesoporous ITO electrode loaded with MP-11 (●) $\Gamma = 3 \times 10^{-10}$ mol.cm^{-2} and (○) $\Gamma = 8 \times 10^{-10}$ mol.cm^{-2} and monitored at $\lambda = 420$ nm during a potential step from 0.1 to -0.8 V (blue line). The data were obtained from the average of repetitive runs using an integration time of (●) 4 or 20 (○) ms. $T = 20$°C; 100 mM HEPES buffer, pH 7.0. Red lines: fit to a single exponential decay with a time constant of 30 ms.

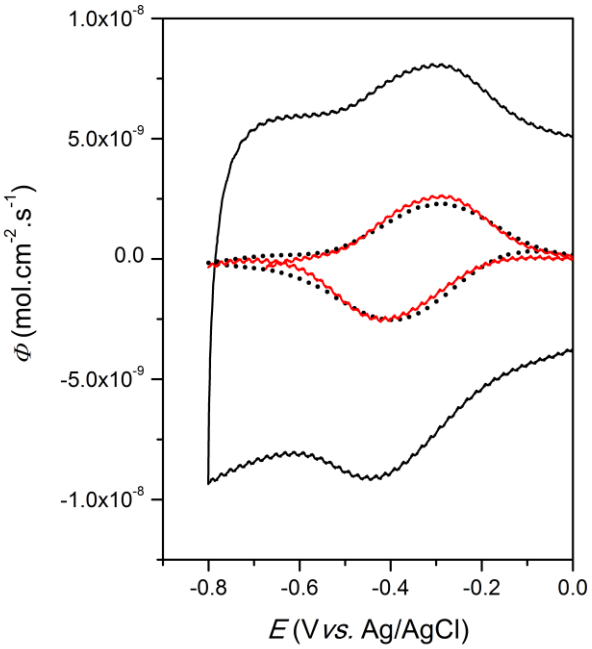

Figure S5: Cyclic voltammogram (black line) and derivative cyclic voltabsorptogram (●) simultaneously recorded at a mesoporous ITO electrode saturated with MP-11 ($\Gamma = 8 \times 10^{-10}$ mol cm^{-2}). The absorbance was monitored at λ = 420 nm and the potential scanned at v = 1 V s^{-1}. The current and absorbance responses were both converted in flux densities using eq 1. Integration time: 20 ms; T = 20°C; 100 mM HEPES buffer, pH 7.0. The red line is the cyclic voltammogram corrected from the capacitive current.